Journal of Colloid and Interface Science 365 (2012) 103–109

Contents lists available at SciVerse ScienceDirect

Journal of Colloid and Interface Science

www.elsevier.com/locate/jcis

Copper nanoparticles incorporated with conducting polymer: Effects of copper concentration and surfactants on the stability and conductivity

Long Quoc Pham [a], Jong Hwa Sohn [a], Chang Woo Kim [a], Ji Hyun Park [b], Hyun Suk Kang [b], Byung Cheol Lee [b], Young Soo Kang [a,*]

[a] Department of Chemistry, Sogang University, #1 Shinsu-dong, Mapo-gu, Seoul 121-742, Republic of Korea
[b] Korea Atomic Energy Research Institute, 1045 Daedeok-daero, Yuseong-Gu, Daejeon 305-353, Republic of Korea

ARTICLE INFO

Article history:
Received 23 June 2011
Accepted 19 September 2011
Available online 24 September 2011

Keywords:
Copper nanoparticles
Conducting polymer
Conducting ink

ABSTRACT

Copper nanoparticles are prepared in aqueous solution by reducing copper ions with hydrazine hydrate in the presence of cetyl trimethylammonium bromide (CTAB) and polyvinylpyrrolydone (PVP) as stabilizers. With only CTAB was used as stabilizer, copper nanoparticles are aggregated and partially oxidized to Cu_2O. When both PVP and CTAB were used, dispersed copper nanoparticles with 56 nm diameter were obtained. Copper nanoparticles are simply mixed with poly (3,4-ethylenedioxythiophene)/poly(styrenesulfonate) (PEDOT/PSS) in aqueous solution to form conducting composite. The effect of copper weight percent and surfactants on the conductivity and stability of the composite has been investigated.

1. Introduction

Due to high conductivity, noble metal nanoparticles (as gold, silver and copper) have been attracted for decades. Among these metals, copper nanoparticles still have more attraction because of the low cost. Recently, gold and silver nanoparticles are widely concerned [1–4], while copper nanoparticles are difficult to be applied because they are easily oxidized in ambient air. To protect copper nanoparticles against oxidation and agglomeration, the synthesis can be done with capping agents by many methods such as chemical reducing process, polyol process, microemulsion, γ – irradiation and thermal decomposition [5–10]. Cationic, anionic or nonionic surfactants and polymers were used as capping agent to protect copper nanoparticles and control the size and shape of the particles [11–14].

Since the discovery in 1977, conjugated polymers have become greatest applications in electronic fields and solar cell [15–17]. Nanocomposites of metal and conducting polymers have received a great attention due to the high potential of the materials for electrocatalysts, chemical sensors and microelectronics [18]. Many studies [19–22] have been focused on the interaction between metals and conjugated polymers to improve the conductivity of the materials as a hybrid conducting ink which has many applications such as inkjet printing, printed circuit, and solar cells. Conjugated polymers, such as polyaniline and polypyrrole, were widely used as materials for hybrid ink. The problem is that those kinds of polymer are hardly soluble in organic solvents. So polymer modification or deposition processes were used to prepare the composite [23–26]. These processes are not proper for preparing copper composite because the copper would be easily oxidized and it is also difficult to control the composition of materials. In this work, the copper nanoparticles were synthesized by chemical reduction and mixed with water soluble conducting polymer PEDOT/PSS to study the conductivity of the incorporated composite by controlling the proportion of the mixing components. We supposed that this method is more convenient than the other kinds of method mentioned above. Here, we report a method to synthesize copper nanoparticles in aqueous solution in the presence of CTAB and PVP. With both PVP and CTAB, the copper nanoparticles are well protected from oxidation. The nanoparticles are well dispersed in ethanol or water, so that they can be easily mixed with PEDOT/PSS in water to form a hydrophilic incorporated paste.

2. Experiment details

2.1. Materials

Copper chloride ($CuCl_2$, 97%), cetyl trimethylammonium bromide (CTAB, 95%), polyvinylpyrrolydone (PVP, M_w = 10.000 g/mol) and hydrazine hydrate ($N_2H_4{\cdot}xH_2O$, $x \sim 1.5$, 50–60%, 1.029 g/ml at 25 °C) were purchased from Aldrich. Ammonia solution (28–30%, 0.89 g/ml at 25 °C) was obtained from Jin Chemical Pharmaceutical Co., Ltd., Korea. For composite preparation, poly (3,4-ethylenedioxythiophene)–poly(styrenesulfonate) solution (PEDOT/PSS, 1.3 wt% in water) and sodium dodecylbenzenesulfonate (SDBS,

* Corresponding author. Fax: +82 2 701 0967.
E-mail address: yskang@sogang.ac.kr (Y.S. Kang).

0021-9797/$ - see front matter © 2011 Elsevier Inc. All rights reserved.
doi:10.1016/j.jcis.2011.09.041

Technical Grade) were obtained from Aldrich. To make comparison, commercial silver nanoparticle powder (99.9%) was purchased from ABC Nanotech Co. Deionized water (DI water) was obtained from Milli-Q Instrument (0.22 μm, Millipore). All chemicals were used without further purification.

2.2. Synthesis of copper nanoparticles

In this process, two equal volume solutions of reactants were prepared: Solution A was prepared by adding 0.555 g of $CuCl_2$ into 100 ml aqueous solution of 0.1 M CTAB (3.64 g) and 1.6×10^{-3} M PVP (1.6 g) to form a 0.04 M copper (II) solution. This solution was bubbled with argon gas to remove oxygen. Then, 1.0 ml of ammonia solution was added to solution A to adjust pH up to 10. In solution B, 100 ml aqueous solution of CTAB and PVP with the same concentrations as solution A was bubbled with argon gas in a capping reactor to remove oxygen and maintain an inert environment. Then, 4 ml of hydrazine hydrate was injected to form a 0.64 M solution of hydrazine. For reaction, solution B was heated to 60 °C in a water bath, and then solution A was injected into solution A dropwise. The mixture was stirred vigorously for 6 h. Temperature was maintained at 60 °C during the reaction time. Copper nanoparticles were separated by centrifugation and washed 3 times with water and ethanol alternately to remove reactants and capping agents and then dried in a vacuum at room temperature for 3 h to yield final product. To study the effect of capping agents, several experiments were carried out with different concentrations of CTAB and PVP. Different reaction temperatures were also applied to get the optimum condition on the temperature effect for the synthesis procedure.

2.3. Preparation of copper paste

A 0.025 g of PEDOT/PSS was mixed with 2.3–3.1 ml of DI water and 0.05–0.25 g of SDBS. The solution was stirred and bubbled with argon gas simultaneously for 1 h. Then, 0.025–0.075 g of synthesized copper powder was added. The paste was stirred vigorously for 12 h under argon flux. Copper composite was coated on glass slide (1×1 cm^2) by spin coating (300 rpm, 1 min). Coated paste was dried in a vacuum for 12 h. Weight percent of copper powder, polymer and SDBS were varied on the range as shown in Table 1 to study their effects on conductivity of paste and to get the optimum one.

2.4. Characterizations and measurements

Copper nanoparticles were characterized by using X-ray powder diffraction (XRD), transmission electron microscopy (TEM), FTIR spectroscopy and UV–Vis spectroscopy. Resistivity of copper paste was measured by using four point probe method, and cross-section of the film was checked by scanning electron microscopy (SEM) to define the thickness of pastes. The XRD patterns of the samples were recorded using the Cu Kα radiation (λ = 1.54056 Å) of a Rigaku X-ray diffractometer operating at 40 kV and 150 mA at a scanning rate of 0.02° per step in the 2θ range of $10° \leqslant 2\theta \leqslant 80°$. TEM was performed on JEOL, JEM-2010 and JEOL JEM 2100F transmission electron microscopes operating at 200 kV. A small amount of the powder sample was dispersed into ethanol (99.9%), and a drop of it was placed over a carbon coated microscopic copper grid (300 mesh size). FTIR spectra were acquired with a Nicolate Avatar 330 Spectrophotometer. The UV–Vis optical absorbance of the nanoparticles was measured using an Agilent 8453 Spectrophotometer. SEM was performed on the field emission scanning electron microscope (FE-SEM) Hitachi S-4300. Resistances of pastes were measured on 2420 3A Source Meter with four point probes. The specific resistance of paste (ρ) was calculated using the following equation [27]:

$$\rho = \frac{2\pi t}{\ln 2}\left(\frac{V}{I}\right)$$

When $R = V/I$ is the value that was read in the measurement instrument, the conductivity is calculated by the following equation:

$$C = \frac{1}{\rho} = \frac{\ln 2}{2\pi t R}$$

where C is the conductivity (S cm^{-1}), t is the thickness of paste film (cm), and R is the resistivity of paste film (Ω).

3. Results and discussion

3.1. Effect of CTAB and PVP concentration

Fig. 1 shows the TEM images of copper nanoparticles synthesized with (a) 0.025 M, (b) 0.05 M and (c) 0.1 M CTAB at 60 °C. At low concentration of CTAB, copper nanoparticles were aggregated (Fig. 1a and b). At the concentration of 0.1 M CTAB, nanoparticles with the size of 50 nm are obtained (Fig. 2c). CTAB is transformed to cetyl trimethylammonium hydroxide (CTAOH) [28] at high pH and binds to copper surface. The electrostatic interaction between oxy in hydroxyl group and positive charge of copper surface prevents the agglomeration of particles. XRD patterns of samples were shown in Fig. 2a–c. The diffraction peaks appearing at 2θ = 43.2, 50.2 and 73.8° correspond to the (1 1 1), (2 0 0), (2 2 0) planes of Cu nanoparticle crystal. The peak at 2θ = 36.3° is assigned to the (1 1 1) plane of cuprous oxide (Cu_2O) crystal. Even though the concentration of CTAB is increased, the peaks of Cu_2O still appear in all samples. CTAB can form micelles in water at concentration higher than the critical micellar concentration (cmc) of 0.1 mM in water at pH = 10 [29]. In the presence of Cu^{2+} ions, the cmc values of CTAB were increased [30]. When adding N_2H_4, Cu^{2+} is reduced to Cu nanoparticles, resulting in the decrease in cmc value. CTAB molecules leave the Cu surface to bind in micelles. Thus, the copper nanoparticles are easily oxidized because of the decrease in CTAB

Table 1
Conductivity of pastes with different compositions. The weight percent values were calculated before mixing.

Content samples	PEDOT/PSS (wt%)	Cu (wt%)	SDBS (wt%)	L conductivity (S cm^{-1})
1	0.5	0	0	9.64×10^{-4}
2	0.5	0.5	1	2.74×10^{-3}
3	0.5	0.5	2	4.63×10^{-4}
4	0.5	0.5	5	3.41×10^{-5}
5	0.5	1	1	7.23×10^{-3}
6	0.5	1	2	8.27×10^{-4}
7	0.5	1	5	5.93×10^{-5}
8	0.5	1.5	1	2.94×10^{-4}
9	0.5	1.5	2	1.38×10^{-5}
10	0.5	1.5	5	4.36×10^{-7}

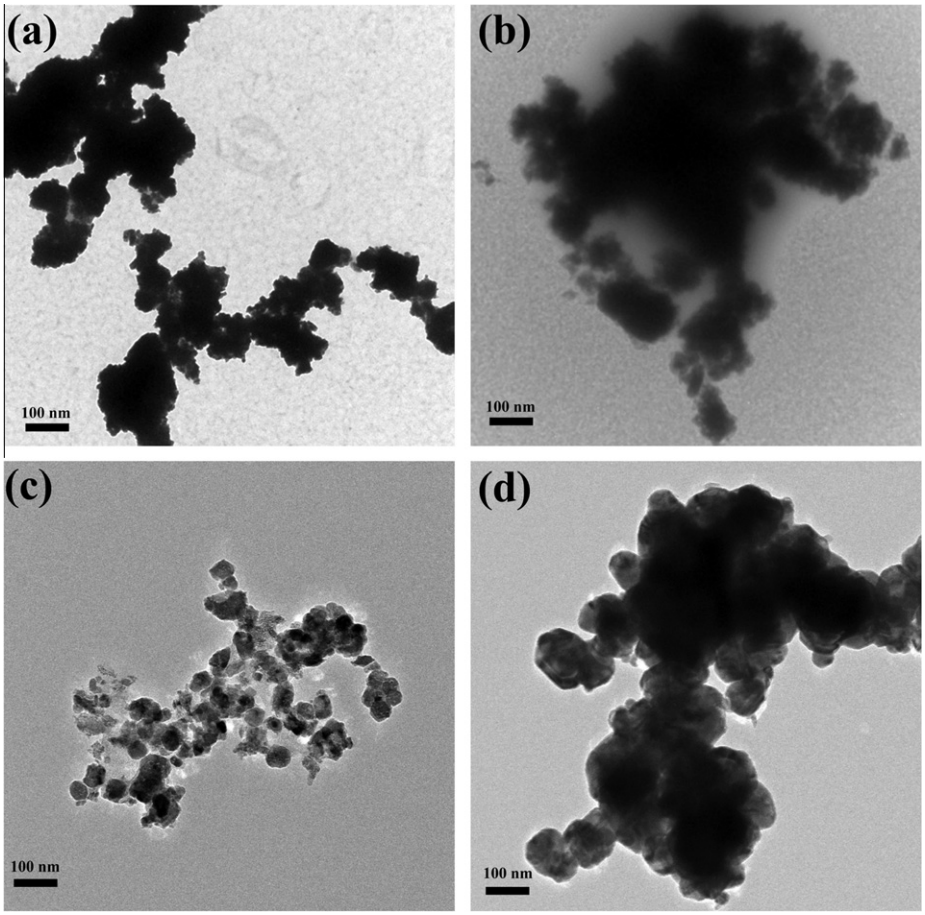

Fig. 1. TEM images of copper nanoparticles with $[CuCl_2]$ = 0.04 M, $[N_2H_4]$ = 0.64 M and (a) 0.025 M CTAB; (b) 0.05 M CTAB; (c) 0.1 M CTAB (d) 1.27×10^{-2} M PVP. Reaction temperature: 60 °C.

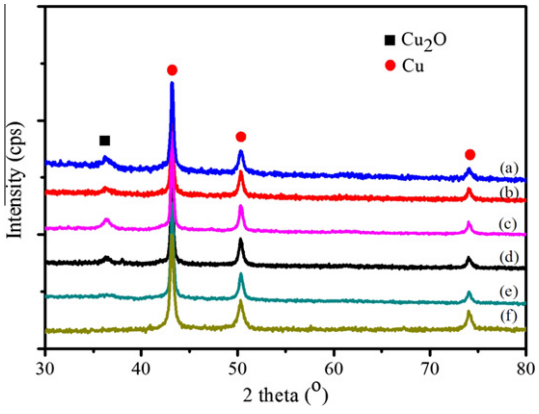

Fig. 2. XRD patterns of copper nanoparticles with different concentrations of CTAB. $[CuCl_2]$ = 0.04 M, $[N_2H_4]$ = 0.64 M and (a) 0.025 M CTAB; (b) 0.05 M CTAB; (c) 0.1 M CTAB (d) 0.1 M CTAB + 4×10^{-4} M PVP (e) 0.1 M CTAB + 8×10^{-4} M PVP (f) 0.1 M CTAB + 1.6×10^{-3} M PVP. Reaction temperature: 60 °C.

concentration on the surfaces. PVP was used to improve the capping effect on copper nanoparticle surface. Fig. 2 shows the XRD patterns of Cu nanoparticles synthesized with 0.1 M of CTAB and different concentrations of PVP. When the concentration of PVP is increased, the peak of Cu_2O in XRD pattern is decreased. And, at the concentration of 1.6×10^{-3} M, there is no peak of Cu_2O in XRD pattern. With large molecular weight of 10,000 g/mol, PVP can cover the CTAB bilayers [31] on the surface of Cu nanoparticles and prevent the formation of micelles (as shown in Scheme 1). The

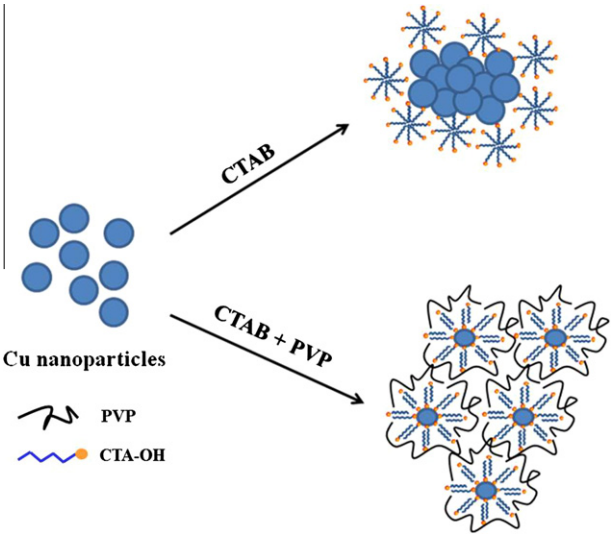

Scheme 1. Schematic drawing of synthesis procedure.

hydroxyl groups with the formation of partial positive surface charge on the metal nanoparticles [32] can bind to the surface of metal nanoparticles more easily than PVP. CTAOH molecule can dominate the formation of bilayers on the surface of copper nanoparticles, and PVP will cover outside. By this way, PVP can restrict the micelle formation of CTAB and protect Cu nanoparticles from

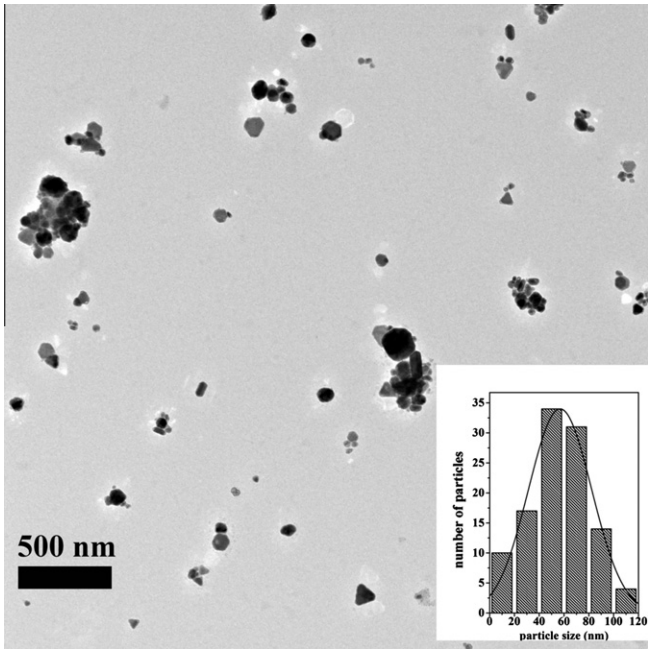

Fig. 3. TEM images and size distribution of PVP–CTAB stabilized copper nanoparticles (average diameter: 56 nm). [$CuCl_2$] = 0.04 M, [N_2H_4] = 0.64 M, [CTAB] = 0.1 M, [PVP] = 1.6×10^{-3} M. Reaction temperature: 60 °C.

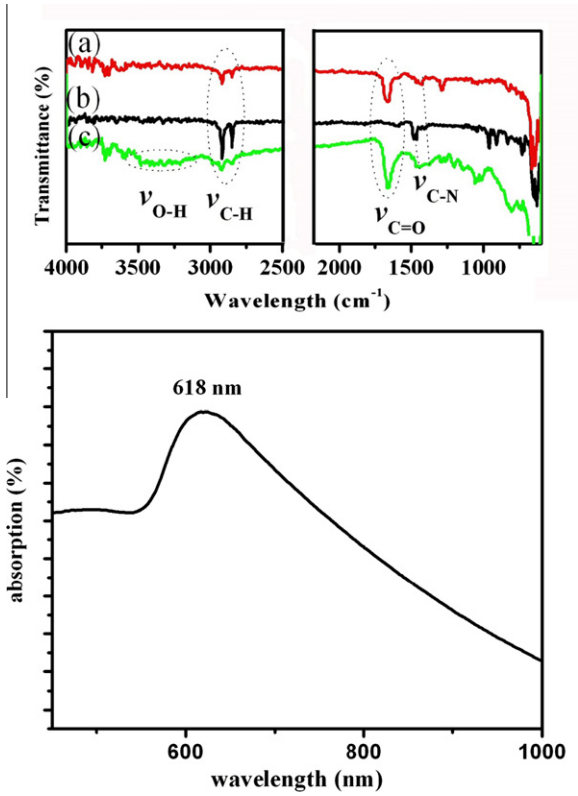

Fig. 4. FTIR spectra of (a) PVP; (b) CTAB; (c) PVP–CTAB stabilized copper nanoparticles (Cu NPs) and UV–Vis absorption of copper nanoparticles in ethanol. [$CuCl_2$] = 0.04 M, [N_2H_4] = 0.64 M, [CTAB] = 0.1 M, [PVP] = 1.6×10^{-3} M. Reaction temperature: 60 °C.

oxidation and agglomeration. Fig. 3 shows the TEM images of Cu nanoparticles synthesized with 0.1 M CTAB and 1.6×10^{-3} M PVP at 60 °C. The dispersion of Cu nanoparticles stabilized by both PVP and CTAB was also better than the one stabilized by only CTAB. Average diameter of copper nanoparticles is 56 nm. We also synthesized copper nanoparticles with only PVP to study the effect of capping agent on controlling particle size and distribution. Fig. 2d shows the TEM image of copper nanoparticles prepared in the presence of PVP at 1.27×10^{-2} M concentration. The synthesis of copper nanoparticles includes two important stages: nucleation from the homogeneous solution and growth of nuclei. As N_2H_4 is a strong reducing agent, the nucleation takes place rapidly in the high growth rate. The growth of copper nuclei is also fast because of the high surface energy of copper nanoparticles. In comparison with CTAB, PVP has longer chain molecules and would give more gaps for the nuclei so the growth of nuclei in PVP is faster than the growth in CTAB. PVP chains also have neutral charge and hydrophilic properties that cannot interact with copper nanoparticles surface as well as CTAB. Thus, all of the particles were agglomerated in bigger size when only PVP is used as shown in Fig. 2d. The presence of CTAB forms bilayers on the surface of copper nanoparticles. These bilayers work as a barrier to the growth of Cu nanoparticles and increase the dispersion of Cu nanoparticles.

Fig. 4 shows the FTIR spectra of (a) PVP, (b) CTAB and (c) CTAB–PVP stabilized Cu nanoparticles. The peaks at 2920 cm^{-1} and 2850 cm^{-1} are assigned to the CH_2 stretching vibrations of alkyl chains in PVP and CTAB. The peaks at 1670 cm^{-1} are assigned to C═O stretching in PVP. The broad peak from 3500 cm^{-1} to 3000 cm^{-1} is assigned to the OH stretching vibration of CTAOH. The peaks at 1478 cm^{-1} and 1430 cm^{-1} are assigned to be C—N vibrations in PVP and CTAB, respectively [30]. Compared with CTAB and PVP spectrum, those peaks in copper sample are little blue shifted. This can be explained by the interaction of PVP and CTAOH with Cu surface. Those peaks appearing in FTIR spectrum of Cu sample matching with those in individual PVP and CTAB indicate the presence of capping layer of PVP and CTAB on the surface of Cu nanoparticles. As the PVP has hydrophilic properties, the copper nanoparticles can be dispersed better in the presence of both PVP and CTAB in aqueous solution than in the presence of only ionic surfactant. This is significant when the copper nanoparticles need to be dispersed in the water medium to prepare pastes with PEDOT/PSS. UV spectrum in Fig. 4 shows the surface plasmon absorption band at 618 nm of copper nanoparticles in ethanol.

3.2. Effect of temperature

The effect of temperature on the synthesis of copper nanoparticles was studied. The reducing process of Cu^{2+} to Cu^0 involves two steps:

$$Cu^{2+} \xrightarrow{e} Cu^{1+} \xrightarrow{e} Cu^0$$

Fig. 5 shows TEM images and XRD patterns of the synthesized Cu nanoparticles at (a) room temperature (RT), (b) 60 °C and (c) 90 °C, respectively. At room temperature, XRD patterns show that Cu_2O was formed on the product while there was no peak of Cu_2O in XRD patterns at higher temperature. This means that the reducing process of copper takes place partially at low temperature and completely done at higher temperatures. However, the increase in temperature would lead to the agglomeration of the copper nanoparticles as shown in Fig. 5.

3.3. Preparation of copper paste

Without using SDBS, the copper paste is easily oxidized after stopping Argon gas flowing in short time. The change of paste color from brown-blue[1] to green-yellow indicates the formation of Cu_2O

[1] For interpretation of color in Fig. 6, the reader is referred to the web version of this article.

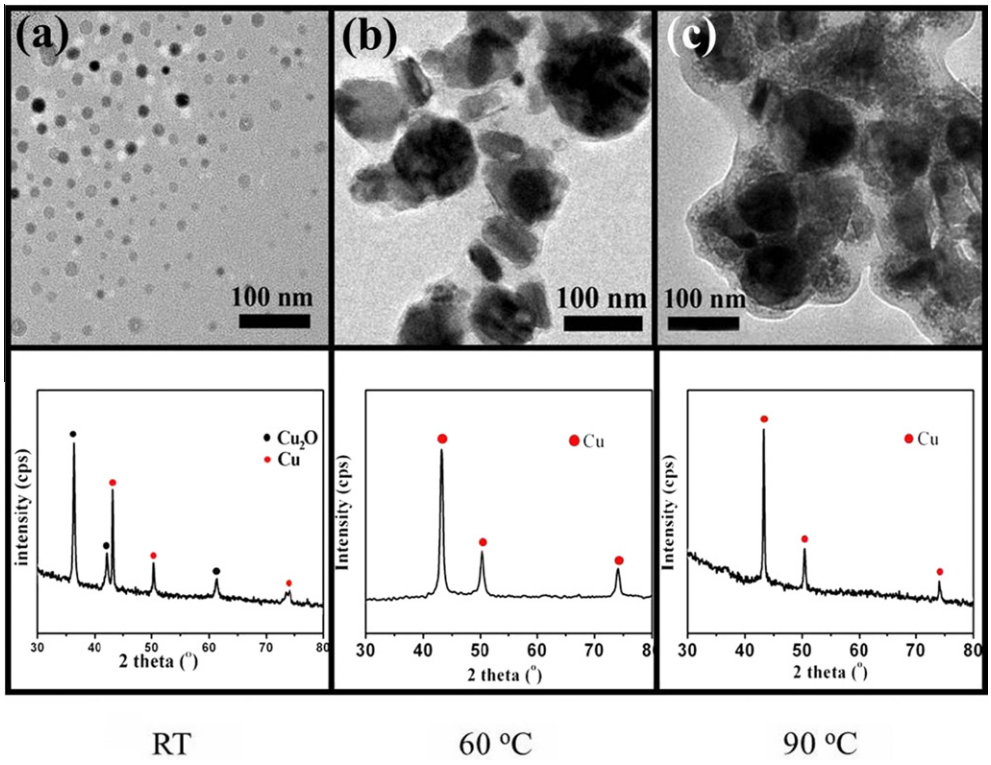

Fig. 5. TEM images and XRD patterns (in column) of samples synthesized at (a) room temperature, (b) 60 °C, (c) 90 °C. $[CuCl_2] = 0.04$ M, $[N_2H_4] = 0.64$ M, [CTAB] = 0.1 M, $[PVP] = 1.6 \times 10^{-3}$ M.

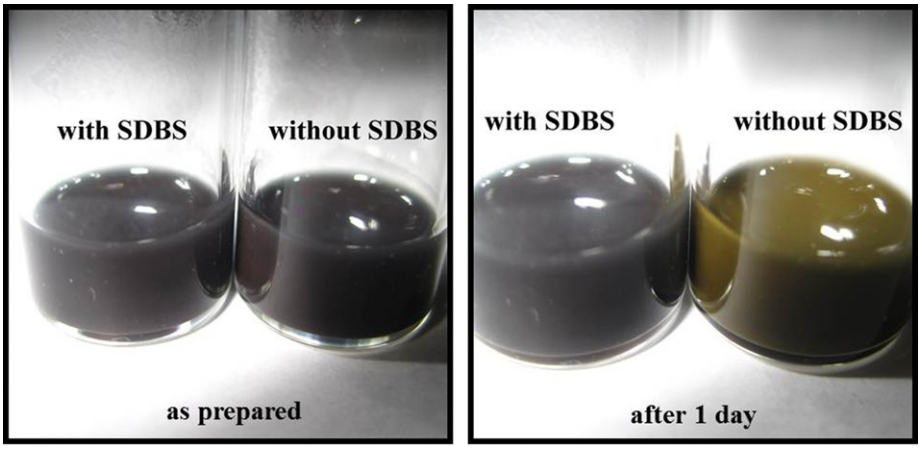

Fig. 6. Color change of copper pastes after exposed in ambient air after 1 day. The color change from gray to yellow indicates the oxidation of copper nanoparticles.

as shown in Fig. 6. The presence of SDBS not only prevents the oxidation but also disperses copper powder into polymer solution. Table 1 presents the conductivity of pastes with different compositions. Fig. 7 displays the specific conductivity of pastes versus SDBS concentration. When the concentration of SDBS is increased from 1 wt% to 5 wt%, conductivity of copper paste is decreased. Surfactants act as barrier of charge transport. The increase in SDBS concentration will decrease the conductivity of solid conducting pastes because of the increased inter-distance and decreased contact area between the particles of the networks in the pastes [33–37]. The paste with 1 wt% of SDBS shows the highest conductivity compared with others. This is fit with what was reported in the work of Wang et al. [38]. The paste of 1 wt% of SDBS is treated at 100 °C for 1 h to remove water completely. There is no significant change in conductivity, indicating that moisture or ionic conducting of SDBS has no effect on the conductivity of paste. The inset in Fig. 7 displays the relationship between specific conductivity of paste with 1 wt% of SDBS and Cu powder/PEDOT-PSS weight ratio (R). The conductivity of paste is increased when the ratio R is increased from 0 to 2/1. Fig. 8 shows the cross-sectional images of paste with $R = 1/1$, $R = 2/1$ and $R = 3/1$. At $R = 1/1$ (equivalent to 25 wt% of copper powder in drying paste), we cannot see the copper particles (Fig. 8a), while we can find copper particles with about 2 μm in $R = 2/1$ (equivalent to 40 wt% of copper powder in drying paste) as shown in Fig. 8b and c. At low weight percent of copper nanoparticles, the amount of SDBS is sufficient to disperse copper nanoparticles into the polymer solution. The surfaces of copper nanoparticles would be covered with a lot of SDBS mole-

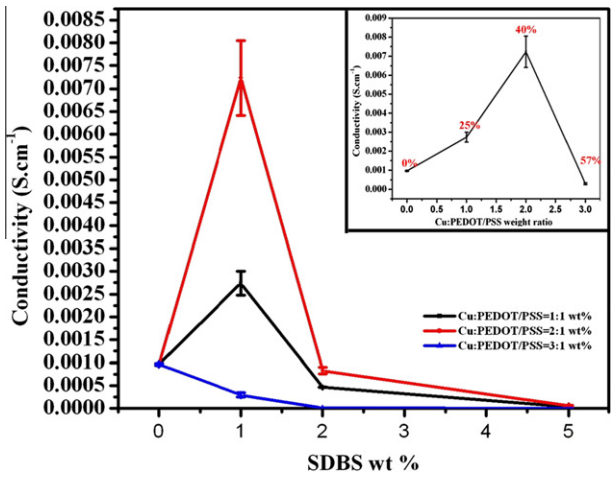

Fig. 7. Relationship between specific conductivity of paste and SDBS weight percent with different weight ratio Cu powder/polymer. Inset: relationship between specific conductivity of paste and weight ratio of Cu powder: polymer at 1% weight of SDBS. The numbers upon each point in the chart describe the weight percent of Copper powder in paste after drying. Cu nanoparticles were obtained at $[CuCl_2] = 0.04$ M, $[N_2H_4] = 0.64$ M, [CTAB] = 0.1 M, [PVP] = 1.6×10^{-3} M. Reaction temperature: 60 °C.

cules as well as CTAB and PVP, so that the contact surface area between copper and polymer is decreased. When the weight percent of copper powder is increased, the thickness of capping layer with SDBS is decreased. Copper nanoparticles would be agglomerated to form bigger size resulting in the larger contact surface area so that conductivity of paste is increased. The drop of conductivity when the weight ratio R is increased to 3/1 (equivalent to 57 wt% of copper powder in drying paste) can be explained by the separation of copper powder from the paste as shown in Fig. 8d. As reported in Lee et al. [39], the metallic nanoparticles are dispersed within the conducting polymer, where the weight ratio of the conducting polymer to the metallic nanoparticles ranges from 1:1 to 3:1. As the weight ratio is increased, mobility of the device comprising the paste formulation decreases. Tani et al. [40] also reported that the high weight percent of copper should cause the break of substrate when copper pastes with more than 60 wt% copper powder were treated at high temperature. In our work, the conducting polymer is not only conductors but also connectors of copper nanoparticles. Thus, this can enhance the conductivity of the paste materials as shown in the results. The use of surfactant with suitable concentration can protect the copper nanoparticles from the oxidation without reducing the conductivity of paste. The copper paste prepared at weight ratio $R = 2/1$ (equivalent to 40 wt% of copper powder in drying paste) with 7.23×10^{-3} S cm^{-1} of conductivity shows the higher conductivity compared with pristine PEDOT/PSS in the previous works (below 10^{-3} S cm^{-1}) at the same condition [41,42]. Although the conductivity of the copper paste prepared in this study is lower than that reported in other metal paste such as gold or silver paste [43,44], the work gives a critical point on the protection of copper nanoparticle ink with surfactants. On the other hands, the preparation is simply carried out at room temperature with fit for copper nanoparticle and easy-decomposed polymer. This method is also economical because the copper precursors are cheap and the copper weight percent is less than 40%. The enhancement of conductivity could be utilized for suitable purposes.

4. Conclusion

In summary, copper nanoparticles with average diameter of 56 nm were synthesized by chemical reduction. PVP and CTAB not only prevent the agglomeration but also protect the copper nanoparticles from the oxidation. The CTAB–PVP stabilized copper nanoparticles can be dispersed in ethanol or water well, and this enables to prepare hydrophilic incorporated materials with PEDOT/PSS. With 1 wt% of SDBS as surfactant, copper composites are more homogeneous and stable in ambient air. The increase in the concentration of surfactant would result in the decrease in conduc-

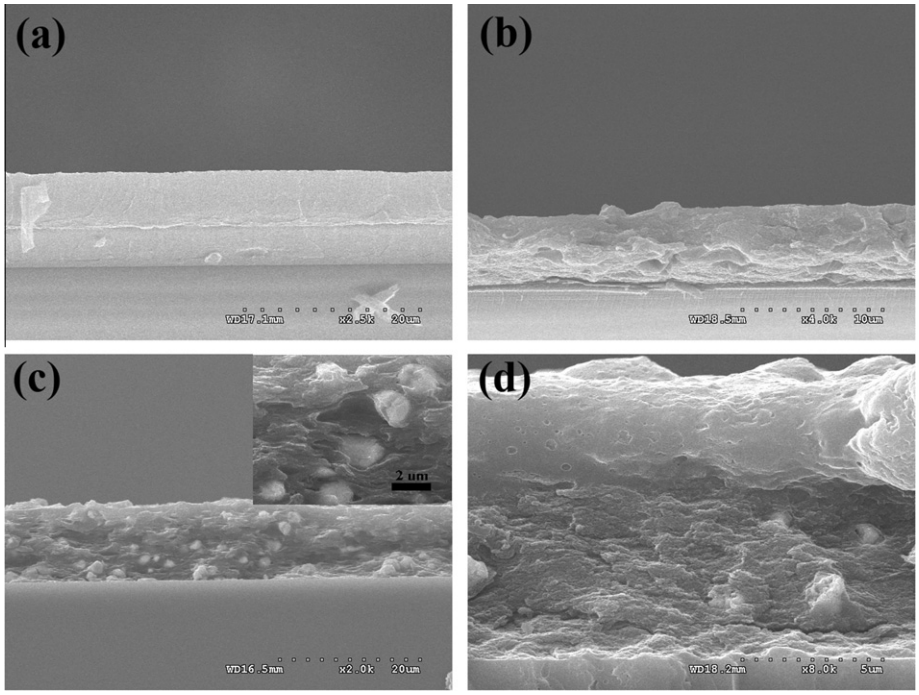

Fig. 8. SEM images of cross-section of pastes with 1% (wt.) of SDBS and different weight percent ratio between Cu powder and PEDOT/PSS (a) 0:1 (b) 1:1 (c) 2:1 (d) 3:1. Cu nanoparticles were obtained at $[CuCl_2] = 0.04$ M, $[N_2H_4] = 0.64$ M, [CTAB] = 0.1 M, [PVP] = 1.6×10^{-3} M. Reaction temperature: 60 °C.

tivity because of the increased inter-particle distances and the decreased contact areas among the Cu nanoparticles. The conducting paste of Cu powder/PEDOT–PSS with weight ratio of 2:1 shows the higher conductivity compared with pristine conducting polymer, while increasing the ratio to 3:1 results in the phase separation and the decrease in conductivity.

Acknowledgment

This research is financially supported by Korean Atomic Energy Research Project from KOSEF.

References

[1] P. Calvert, Chem. Mater. 13 (2001) 3299.
[2] K. Woo, D. Kim, J.S. Kim, S. Lim, J. Moon, Langmuir 25 (2009) 429.
[3] L.M. Davis, D.W. Thompson, Chem. Mater. 19 (2007) 2299.
[4] Y.H. Kim, D.K. Lee, H.G. Cha, C.W. Kim, Y.C. Kang, Y.S. Kang, J. Phys. Chem. B 110 (2006) 24923.
[5] X. Su, J. Zhao, H. Bala, Y. Zhu, Y. Gao, S. Ma, Z. Wang, J. Phys. Chem. C 111 (2007) 14689.
[6] B.K. Park, S. Joeng, D. Kim, J. Moon, S. Lim, J. Kim, J. Colloid Interface Sci. 311 (2007) 417.
[7] S. Panigrahi, S. Kundu, S. Basu, S. Praharaj, S. Jana, S. Pande, S.K. Ghosh, A. Pal, T. Pal, J. Phys. Chem. C 111 (2007) 1612.
[8] F. Zhou, R. Zhou, X. Hao, X. Wu, W. Rao, Y. Chen, D. Gao, Radiat. Phys. Chem. 77 (2008) 169.
[9] Z. Liu, Y. Yang, J. Liang, Z. Hu, S. Li, S. Peng, Y. Qian, J. Phys. Chem. B 107 (2003) 12658.
[10] Y.H. Kim, D.K. Lee, B.G. Jo, J.H. Jeong, Y.S. Kang, Colloids Surf., A: Physicochem. Eng. Aspects 284–285 (2006) 364.
[11] A. Athawale, P. Katre, M. Kumar, M.B. Majumdar, Mater. Chem. Phys. 91 (2005) 507.
[12] P. Kanninen, C. Johans, J. Merta, L. Kontturi, J. Colloid Interface Sci. 318 (2008) 88.
[13] A. Sarkar, T. Mukherjee, S. Kapoor, J. Phys. Chem. C 112 (2008) 3334.
[14] S. Chen, J.M. Sommer, J. Phys. Chem. B 105 (2001) 8816.
[15] H. Shirakawa, E.J. Louis, E.J. MacDiarmid, C.K. Chiang, A.J. Heeger, J. Chem. Soc., Chem. Commun. 579 (1977).
[16] F. Schindler, J.M. Lupton, J. Muller, J. Feldmann, U. Scherf, Nat. Mater. 5 (2006) 141.
[17] M.K. Coakley, D.M. McGehee, Chem. Mater. 16 (2004) 4533.
[18] M. Singh, H.M. Haverinen, P. Dahgat, J.E. Jabbour, Adv. Mater. 22 (2010) 6.
[19] S.H. Cho, S.M. Park, J. Phys. Chem. B 110 (2006) 25656.
[20] K. Park, K. Seo, J. Lee, Colloids Surf., A: Physicochem. Eng. Aspects 313–314 (2008) 351.
[21] P. Englebienne, A.V. Hoonacker, J. Colloid Interface Sci. 292 (2005) 445.
[22] C.S. Izumi, G.S. Andrade, M.A. Temperini, J. Phys. Chem. B 112 (2008) 16334.
[23] M.M. Oliveira, E.G. Castro, D.C. Canestaro, D. Zanchet, D. Ugaret, S.L. Roman, A.G. Zarbin, J. Phys. Chem. B 110 (2006) 17063.
[24] J.M. Pringle, O.W. Jensen, C. Lynam, G.G. Wallace, M. Forsyth, D.R. MacFarlane, Adv. Funct. Mater. 18 (2008) 2031.
[25] A.K. Nandi, P. Mukherjee, A. Dawn, Langmuir 23 (2007) 5231.
[26] D. Schemeiβer, G. Appel, R.P. Mikalo, Synth. Met. 122 (2001) 91.
[27] A.P. Shuetze, W. Lewis, C. Brown, W.J. Green, Am. J. Phys. 72 (2004) 149.
[28] V.K. Balskrishnan, X. Han, G.W. VanLoon, J.M. Dust, J. Toullec, E. Buncel, Langmuir 20 (2004) 6586.
[29] B.D. Fleming, S. Biggs, E.J. Wanless, J. Phys. Chem. B 105 (2001) 9537.
[30] T. Jakashima, T. Fujiwara, Anal. Sci. 17 (2001) i1241.
[31] B. Nikoobakht, M.A. El-Sayed, Langmuir 17 (2001) 6368.
[32] K.J. Klabunde, Nanoscale materials in chemistry (2002) 29 (Chapter 1).
[33] Y. Joseph, I. Besnard, M. Rosenberger, B. Guse, H.G. Nothofer, J.M. Wessels, U. Wild, A.K. Gericke, D. Su, R. Schloegl, A. Yasuda, T. Vossmeyer, J. Phys. Chem. B 107 (2003) 7406.
[34] B.C. Sih, M.O. Wolf, Chem. Commun. 27 (2005) 3375.
[35] S. Chen, R.W. Murray, S.W. Feldberg, J. Phys. Chem. B 102 (2008) 9898.
[36] A.J. Makinen, I.G. Hill, R. Shashidhar, N. Nikolov, Z.H. Kafafi, Appl. Phys. Lett. 79 (2001) 557.
[37] T.A. Stotheim, J.R. Reynolds, Handbook of Conducting Polymers: Conjugated Polymers – Theory, Synthesis, Properties, and Characterization, 2007 (Chapters 15 and 19).
[38] J. Wang, J. Sun, L. Gao, Y. Liu, Y. Wang, J. Zhang, H. Kajiura, Y.M. Li, K. Noda, J. Alloy. Compd. 485 (2009) 456.
[39] T.C. Lee, B.K. Nelson, C.P. Gerlach, D.E. Vogel, US Patent No. 20080187651 (2008).
[40] H. Tani, Nagaokakyo, K. Honma, Shiga US Patent No. 5336301 (1993).
[41] A.M. Nardes, M. Kemerink, R.J. Janssen, J.A. Bastiaansen, N.M. Kiggen, B.W. Langeveld, A. Breemen, M.M. Kok, Adv. Mater. 19 (2007) 1196.
[42] J. Huang, P. Miller, J.S. Wilson, A.J. Mello, J.C. Mello, D.D. Bradley, Adv. Funct. Mater. 15 (2005) 290.
[43] M.A. Breimer, G. Yevgeny, S. Sy, O.A. Sadik, Nano Lett. 1 (2001) 305.
[44] L. Polavarapu, K.K. Manga, H.D. Cao, K.P. Loh, Q.-H. Xu, Chem. Mater. 23 (2011) 3273.